



# LUND UNIVERSITY

## Carbon Nanotube Emissions from Arc Discharge Production: Classification of Particle Types with Electron Microscopy and Comparison with Direct Reading Techniques.

Ludvigsson, Linus; Isaxon, Christina; Nilsson, Patrik; Tinnerberg, Håkan; Messing, Maria; Rissler, Jenny; Skaug, Vidar; Gudmundsson, Anders; Bohgard, Mats; Hedmer, Maria; Pagels, Joakim

*Published in:*  
Annals of Occupational Hygiene

*DOI:*  
[10.1093/annhyg/mev094](https://doi.org/10.1093/annhyg/mev094)

2016

[Link to publication](#)

*Citation for published version (APA):*

Ludvigsson, L., Isaxon, C., Nilsson, P., Tinnerberg, H., Messing, M., Rissler, J., Skaug, V., Gudmundsson, A., Bohgard, M., Hedmer, M., & Pagels, J. (2016). Carbon Nanotube Emissions from Arc Discharge Production: Classification of Particle Types with Electron Microscopy and Comparison with Direct Reading Techniques. *Annals of Occupational Hygiene*, 60(4), 493-512. <https://doi.org/10.1093/annhyg/mev094>

*Total number of authors:*  
11

### General rights

Unless other specific re-use rights are stated the following general rights apply:  
Copyright and moral rights for the publications made accessible in the public portal are retained by the authors and/or other copyright owners and it is a condition of accessing publications that users recognise and abide by the legal requirements associated with these rights.

- Users may download and print one copy of any publication from the public portal for the purpose of private study or research.
- You may not further distribute the material or use it for any profit-making activity or commercial gain
- You may freely distribute the URL identifying the publication in the public portal

Read more about Creative commons licenses: <https://creativecommons.org/licenses/>

### Take down policy

If you believe that this document breaches copyright please contact us providing details, and we will remove access to the work immediately and investigate your claim.

LUND UNIVERSITY

PO Box 117  
221 00 Lund  
+46 46-222 00 00



# Carbon Nanotube Emissions from Arc Discharge Production: Classification of Particle Types with Electron Microscopy and Comparison with Direct Reading Techniques

Linus Ludvigsson<sup>1,2\*</sup>, Christina Isaxon<sup>2</sup>, Patrik T. Nilsson<sup>2</sup>, Hakan Tinnerberg<sup>3</sup>, Maria E. Messing<sup>1</sup>, Jenny Rissler<sup>2</sup>, Vidar Skaug<sup>4</sup>, Anders Gudmundsson<sup>2</sup>, Mats Bohgard<sup>2</sup>, Maria Hedmer<sup>3</sup> and Joakim Pagels<sup>2</sup>

1.Solid State Physics, Lund University, SE-22100 Lund, Sweden;

2.Ergonomics and Aerosol Technology, Lund University, SE-22100 Lund, Sweden;

3.Occupational and Environmental Medicine, Lund University, SE-22100 Lund, Sweden;

4.National Institute of Occupational Health, P.O. Box 8149 Dep, 0033 Oslo, Norway

\*Author to whom correspondence should be addressed. Tel: +46 (0)46 222 7689; fax: +46 (0)46 222 3637;  
e-mail: [linus.ludvigsson@ftflth.se](mailto:linus.ludvigsson@ftflth.se)

Submitted 2 October 2014; revised 2 December 2015; revised version accepted 7 December 2015.

## ABSTRACT

**Introduction:** An increased production and use of carbon nanotubes (CNTs) is occurring worldwide. In parallel, a growing concern is emerging on the adverse effects the unintentional inhalation of CNTs can have on humans. There is currently a debate regarding which exposure metrics and measurement strategies are the most relevant to investigate workplace exposures to CNTs. This study investigated workplace CNT emissions using a combination of time-integrated filter sampling for scanning electron microscopy (SEM) and direct reading aerosol instruments (DRIs).

**Material and Methods:** Field measurements were performed during small-scale manufacturing of multi-walled carbon nanotubes using the arc discharge technique. Measurements with highly time- and size-resolved DRI techniques were carried out both in the emission and background (far-field) zones. Novel classifications and counting criteria were set up for the SEM method. Three classes of CNT-containing particles were defined: type 1: particles with aspect ratio length:width >3:1 (fibrous particles); type 2: particles without fibre characteristics but with high CNT content; and type 3: particles with visible embedded CNTs.

**Results:** Offline sampling using SEM showed emissions of CNT-containing particles in 5 out of 11 work tasks. The particles were classified into the three classes, of which type 1, fibrous CNT particles contributed 37%. The concentration of all CNT-containing particles and the occurrence of the particle classes varied strongly between work tasks. Based on the emission measurements, it was assessed that more than 85% of the exposure originated from open handling of CNT powder during the *Sieving, mechanical work-up, and packaging* work task. The DRI measurements provided complementary information, which combined with SEM provided information on: (i) the background adjusted emission

concentration from each work task in different particle size ranges, (ii) identification of the key procedures in each work task that lead to emission peaks, (iii) identification of emission events that affect the background, thereby leading to far-field exposure risks for workers other than the operator of the work task, and (iv) the fraction of particles emitted from each source that contains CNTs.

**Conclusions:** There is an urgent need for a standardized/harmonized method for electron microscopy (EM) analysis of CNTs. The SEM method developed in this study can form the basis for such a harmonized protocol for the counting of CNTs. The size-resolved DRI techniques are commonly not specific enough to selective analysis of CNT-containing particles and thus cannot yet replace offline time-integrated filter sampling followed by SEM. A combination of EM and DRI techniques offers the most complete characterization of workplace emissions of CNTs today.

**KEYWORDS:** APS; arc discharge, carbon nanotubes; counting rules; direct reading instruments; NOAA; workplace exposure

## INTRODUCTION

Carbon nanotubes (CNTs) were discovered in 1991 (Iijima, 1991). Since then they have gained special interest due to their unique properties. CNTs can consist of either a single graphene cylinder (single-walled CNTs or SWCNTs) or multiple graphene cylinders (multi-walled CNTs or MWCNTs). CNTs can improve properties like durability, strength, flexibility, and electrical and thermal conductivities (Köhler *et al.*, 2008; Wohlleben *et al.*, 2011; Liu and Kumar, 2014) and can thus be incorporated in different materials such as composites, rubbers, plastics, concrete, and fabrics. The increasing demand for CNTs means increased handling and, inevitably, increased risk of occupational exposure to workers. CNTs are high aspect ratio nanomaterials with low density, high surface-to-mass ratio, and are biopersistent in the lungs (Muller *et al.*, 2005), all of which are properties of hazardous nanomaterials. The fibre-like morphological similarity of many CNTs with asbestos is apparent and the need for a proactive approach to the potential risks is indisputable (Sanchez *et al.*, 2010; Murphy *et al.*, 2011).

Inhalation has been identified as the major exposure route (Hedmer *et al.*, 2013; Ma-Hock *et al.*, 2009, 2013; Pauluhn, 2010a; Gustavsson *et al.*, 2011). To the best of our knowledge no toxicological data for human exposure to CNTs currently exists, but animal inhalation studies of both long and short MWCNTs have been shown to have adverse effects in the lungs, such as inflammation, granuloma formation, and fibrosis (Mercer *et al.*, 2010; Ma-Hock *et al.*, 2013; Pauluhn, 2010b; Murphy *et al.*, 2011). It has also been shown in animals that inhalation exposure to some forms of MWCNTs can promote lung cancer (Sargent *et al.*, 2014).

No legally enforced occupational exposure limits (OELs) for CNTs exist, but there are proposals for a benchmark exposure limit for airborne fibrous nanomaterials (e.g. CNTs) with high aspect ratios (>3:1 and length >5  $\mu\text{m}$ ) set at 0.01 fibre  $\text{cm}^{-3}$  from national organizations such as the British Standards Institute (BSI, 2007) and the Institute for Occupational Safety and Health of the German Social Accident Insurance (IFA, 2014). An OEL based on elemental carbon (EC) at 1  $\mu\text{g cm}^{-3}$  as a respirable mass 8-h time-weighted average (TWA-8) concentration has been proposed (NIOSH, 2013).

As long as the research community has not agreed on what dose metric best correlates with the toxicological effects of CNTs, it is crucial to use a multi-metric approach for emission and exposure measurements. One important metric is the particle number concentration of CNT-containing particles achieved by filter-based air sampling methods in combination with electron microscopy (EM) analysis. EM has previously been used in exposure assessment studies (Ogura *et al.*, 2011; Takaya *et al.*, 2012), but there are currently no standardized methods for measuring and counting CNTs on filter samples. The methods used for CNT counting so far are based on the ones for asbestos counting initially set up by WHO (1986, 1997), examples of which are the NIOSH methods 7400 and 7402. Some studies have followed the NIOSH method 7402 (Han *et al.*, 2008; Bello *et al.*, 2008; Lee *et al.*, 2010). Dahm *et al.* (2012) used a modified the NIOSH method 7402, by excluding the steps required for asbestos identification in the EM analysis. It is important to make both full-shift personal exposure measurements (for comparison with suggested exposure limits), and work task-based

emission measurements (to identify the processes in which emissions occur) so that a complete and accurate evaluation of the exposure risk can be performed. Methner *et al.* (2010) have suggested the nanoparticle emission assessment technique (NEAT), based on a combination of direct reading instrumentation (DRI) and filter-based air samples that is both source specific and in the personal breathing zone (PBZ).

In this study, we focus on characterizing airborne emissions of CNT-containing particles during different work tasks and we utilize both real-time aerosol instruments and filter-based air sampling methods. With the DRIs, it is possible to differentiate between background and process-related nanoparticles and to identify the part of a work task that leads to emissions, but they are commonly not specific enough to selectively analyze CNT-containing particles.

So far, most CNT emission and exposure measurements have been performed in facilities where CNTs are produced by chemical vapor deposition (CVD) (Maynard *et al.*, 2004; Bello *et al.*, 2008; Han *et al.*, 2008; Tsai *et al.*, 2009; Lee *et al.*, 2010; Kumar and Ando, 2010). Another method for CNT generation is the arc discharge technique, which is an inexpensive way of producing high-quality CNTs without the use of metal catalysts. The drawback is a high amount of graphite impurities. To the best of our knowledge, there are no published studies of workplace emissions and exposures during CNT production with the arc discharge technique.

The objectives of this study were: (i) to develop and apply a method based on EM for the classification of airborne CNT-containing particles including agglomerates, (ii) to characterize the emissions of CNTs during different stages of production with the arc discharge technique and during purification and functionalization, (iii) to investigate added values by combined characterization with the SEM technique and highly time- and size-resolved direct reading techniques

## MATERIAL AND METHODS

### Study design

Particle emissions and personal exposure were measured at a small-scale manufacturer that produced MWCNTs with the arc discharge technique. Emission measurements with DRIs and filter sampling were

carried out during manufacturing divided into 11 work tasks performed at designated locations (numbered 1–11 in Tables 1 and 3 and Fig. 1). The facility was divided into three areas denoted as the *production laboratory*, *sieving laboratory*, and *purification laboratory*. The *production and sieving laboratories* were adjacent, connected by an open door during the measurements. The *purification laboratory* was situated on a different floor. A schematic layout of the workplace is provided in Fig. 1.

The measurements were carried out during two consecutive days, the first day in the *production and sieving laboratories* (Work Tasks Nos. 1–6) and the second day in the *purification laboratory* (Work Tasks Nos. 7–11). Emission measurements were carried out in close vicinity of the source (<10 cm; near-field), using both filter samplers and DRIs to measure the immediate emissions. Simultaneous measurements were carried out with the DRIs in the background zone (>3 m from source; far-field). In addition, full-shift personal exposure measurements were carried out, as described in detail by Hedmer *et al.* (2014).

### Method of production and description of work tasks

The arc discharge method produces MWCNTs by means of a continuous electrical discharge between two graphite electrodes within a closed reaction chamber (Gamaly and Ebbesen, 1995). The discharge evaporates the electrode material from the anode followed by deposition on the opposite electrode—the cathode or counter electrode. The core of the deposited material contains the CNTs but also high amounts of carbonaceous impurities and needs to be purified.

After the reaction is completed, there is the *Opening of the reactor* (Work Task No. 3 in Fig. 1) and *Cleaning of the reactor* (Work Task No. 4) by blowing high pressure air into it. After removing the CNT-enriched electrodes a table saw is used for *Cleaving of deposits* (Work Task No. 1) and *Harvesting* (Work Task No. 2) of the CNT-rich material is carried out manually.

The core material is further dispersed in the *sieving laboratory* and sorted with a stack sieve. *Sieving, mechanical work-up, and packaging* (Work Task No. 5) is conducted in a room adjacent to the *production laboratory*. The process, which is not enclosed, is performed by automated shaking of the stack of sieves. No pressurized air is used. The fractions of desired size are selected and this material is labeled 'As produced'. In the same room,

Table 1. List of work tasks performed during production and purification of CNTs and sampling time/length of work task

| Work task                                    | Task number/<br>location in Fig. 1 | Description of sampled work task  | CNT-containing material<br>handled during work task | Sampling time<br>(min) |
|--|------------------------------------|---|---|------------------------|
| Cleaving of deposits<br>(morning)            | 1                                  | Generated deposits/electrodes cleaved<br>with a table saw   | Yes   | 11                     |
| Cleaving of deposits<br>(afternoon)          | 1                                  | Generated deposits/electrodes cleaved with a<br>table saw   | Yes   | 13                     |
| Harvesting                                   | 2                                  | CNT material is harvested from the<br>cleaved electrodes.   | Yes   | 17                     |
| Opening of the reactor                       | 3                                  | The reactor is opened after finished<br>production  | Yes   | 8                      |
| Cleaning of the reactor<br>parts I and II    | 4                                  | High pressure air is blown into the<br>closed reactor. A vacuum cleaner is used to<br>draw air out of the reactor   | No  | 8+4                    |
| Sieving, mechanical<br>work-up and packaging | 5                                  | Harvested material is dispersed and placed in<br>flasks with a magnetic stirrer. The material is then<br>funnelled through a stack sieve. Several iterations<br>are performed | Yes   | 53                     |
| Lathe machining                              | 6                                  | Graphite electrodes are prepared for production<br>using a lathe machine. Visible chunks of graphite<br>are released to air   | No  | 13                     |
| Purification part I                          | 7                                  | Chemical purification in several steps; a furnace was<br>opened during the task   | Yes   | 63                     |
| Purification part II                         | 8                                  | Activities performed inside a fume hood   | Yes   | 70                     |
| Functionalization part I                     | 9                                  | Activities performed inside a fume hood   | Yes   | 13                     |
| Functionalization part II                    | 10                                 | Activities performed inside a fume hood   | Yes   | 24                     |
| Grinding                                     | 11                                 | Coarse functionalized material was ground with mortar<br>and pestle. Ground material was poured into a vial   | Yes   | 35                     |

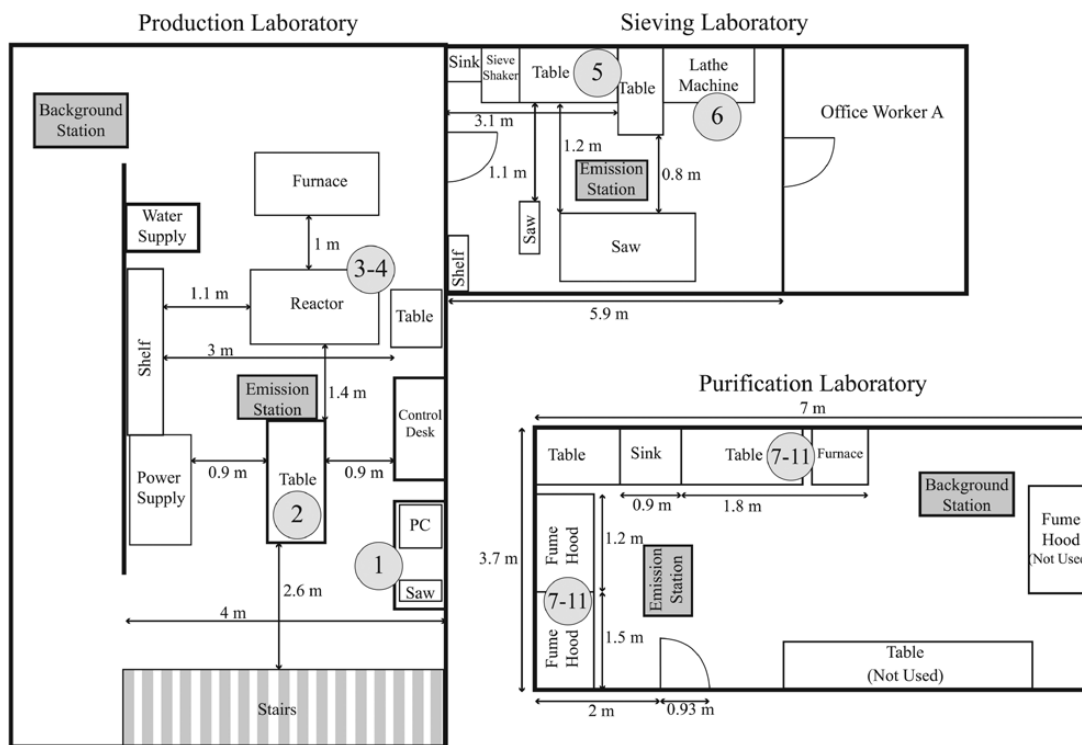


Figure 1 Schematic layout of the facility. Numbers in grey circles correspond to work tasks in Table 1. The production and sieving laboratories were located on a different floor from the purification laboratory.

the graphite electrodes used for the production process are prepared by *Lathe machining* (Work Task No. 6) to fit in electrode holders inside the reactor.

The ‘As produced’ material is further processed in the *purification laboratory*, where it follows a series of steps from raw material to purified CNTs. The purification process involves dispersion of the material in a liquid and several steps of chemical purification. The material is dried in a furnace. Some of the purified material is used for production of functionalized CNTs. The processes of *Purification I and II*, *Functionalization I and II*, and *Grinding* are performed on location/Work Tasks Nos. 7–11 in Fig. 1 and Table 1.

#### Direct reading techniques and filter collection

A summary of the particle sampling techniques and sample locations is given in Table 2. The DRI techniques are described in detail in Table 2 and Supplementary material. Briefly, two aerodynamic particle sizers (APS) were used to measure number concentration and size distributions in the large particles range ( $dp > 0.5 \mu\text{m}$ ). For the small particle

range ( $dp > 0.01 \mu\text{m}$ ), a condensation particle counter (CPC) measured the total number concentration in the emission zone, and a scanning mobility particle sizer (SMPS) provided particle size distributions and total particle number concentrations in the background zone. The APS and CPC used a time resolution of 5 s and the SMPS 180 s. The location of the emission and background measurement stations, listed in Table 2, can be seen in the schematic of the facility in Fig. 1. Sampling was carried out continuously in the background station, throughout the work shift.

Respirable fractions of particles in the emission zone were collected for SEM analysis during each work task. Workers also carried filter samplers in the breathing zone for SEM analysis; sampling took place throughout the full work shift. Two full-shift filter samples were collected each day, one from the worker in the *production* and *sieving laboratories*, and one swapped between the two workers in the *purification laboratory*. Further descriptions of the personal exposure measurements and methods are provided by Hedmer et al. (2014).

**Table 2. List of DRIs and filter-based sampling equipment used in the emission measurements during production and purification of CNTs**

| Instrument/equipment  | Measured/collected size range                         | Location                            | Sample flow (l min <sup>-1</sup> ) |
|---|---|-------------------------------------|------------------------------------|
| Aerodynamic particle sizer (APS 3321 TSI)                                     | Size distribution: >0.5 µm (aerodynamic diameter)     | Emission and background (two units) | 1.0 (5.0)                          |
| Condensation particle counter (CPC 3022 TSI)                                  | Total nbr. conc. >0.007 µm                            | Emission                            | 0.3                                |
| Respirable sampling on polycarbonate membrane filter followed by SEM analysis | 0.04 (geometric diameter)–4 (aerodynamic diameter) µm | Emission, personal breathing zone   | 2.2                                |
| Scanning mobility particle sizer (SMPS Model 3071 TSI)                        | Size distribution: 0.010–0.51 µm (mobility diameter)  | Background                          | 1.0 (sheath air 6.0)               |

Respirable samples were collected on 37-mm track-etched polycarbonate membrane filters with a pore size of 0.4 µm (Nuclepore™ product no. 225–1609, SKC Inc., Eighty Four, PA, USA) using cyclones (BGI4L, BGI Inc., Waltham, USA) mounted in plastic three-piece filter cassettes. A sample flow rate of 2.2 l min<sup>-1</sup> was provided by an Escort ELF pump (MSA, Pittsburgh, PA, USA). The flow rate was checked prior to and after sampling by a primary calibrator (TSI Model 4100, TSI Inc., Shoreview, MN, USA).

Sampling of CNTs using cyclones is recommended by NIOSH (2013). Jones (2005) have shown that the sampling of respirable fibres and particles results in accurate and reliable sampling for the cyclone used as penetration, e.g. depends solely on fibre diameter, independent of fibre length through the cyclone and also led to an even distribution on the filter downstream the cyclone. This observation is important because orientation effects can potentially cause large differences in the aerodynamic diameters assigned for different measurement techniques. The use of respirable sampling may result in the exclusion of some larger CNT-containing agglomerate particles that would have had a low probability to reach the target (pulmonary) region.

### Data analysis

#### *Background correction and averaging for DRIs*

We subtracted the background particles that were not emitted from the work tasks for the DRIs in two different ways. Spatial background subtraction denotes

the difference between the instrument in the emission zone and the instrument at the background station for the same measurement period. Temporal background subtraction denotes the difference between the work task period of the measurement and a three minute period before the work task for the same instrument. Spatial background subtraction was only carried out for the APS measurements, while the temporal background subtraction is given for both the APS and the CPC. The negative values as seen in Table 3 should be interpreted as no significant increase of the average concentration; similarly, increases by less than about 20% relative to the background may be due to variability in the background concentration. The values reported from the DRIs are averages of the periods that were defined as work tasks. The periods are marked in Fig. 2.

#### *SEM method for classifying and counting airborne CNTs*

Most airborne CNTs do not have the typical fibre dimensions required by WHO (length > 5 µm and length:width ratio >3:1) due to agglomeration (Dahm *et al.*, 2012). Consequently, we decided not to apply the WHO standard fibre counting method and instead develop an electron microscopic method for the analysis of airborne CNTs. We manually counted all CNT-containing particles imaged by SEM. If several fibres were attached to or constituted a particle, it was counted as *one* CNT-containing particle. This differs from how asbestos is counted (OH Learning, 2010).

Table 3. Emission concentrations from DRI instruments and results of SEM analysis from all work tasks. Shaded columns are background corrected; clear columns are total particle concentrations (respirable fractions) including background particles. Temporal background corrected denotes adjustment relative to a background period from the same instrument before the task. Spatial background corrected denotes adjustment relative to the simultaneous background measurement with an identical instrument

| Work Task                                     | Location<br>in Fig. 1 | Direct reading instruments  |   |   | SEM analysis                                   |                                       |                  |                    |
|---|-----------------------|---|---|---|--|---------------------------------------|------------------|--------------------|
|   |                       | >0.01 $\mu\text{m}$<br>(CPC) temporal<br>background<br>corrected <sup>a</sup> | >0.5 $\mu\text{m}$<br>(APS)<br>temporal<br>background<br>corrected <sup>a</sup> | >0.5 $\mu\text{m}$ (APS)<br>spatial<br>background<br>corrected <sup>b</sup> | Total<br>(35 nm–4 $\mu\text{m}$ ) <sup>c</sup> | CNT-containing particles <sup>d</sup> | LOD <sup>e</sup> |                    |
|   |                       | # $\text{cm}^{-3}$  | # $\text{cm}^{-3}$  | # $\text{cm}^{-3}$  | # $\text{cm}^{-3}$                             | All types<br># $\text{cm}^{-3}$       | Types (1, 2, 3)% | # $\text{cm}^{-3}$ |
| Cleaving of deposits<br>(morning   afternoon) | 1                     | 39 (1239)  <br>-110(6185)   | 53 (1.7)  <br>93 (4.1)  | 51(2.3)  <br>89(3.7)  | 190 $\pm$ 5.0                                  | <b>1.6 <math>\pm</math> 0.40</b>      | 12, 6, 82        | 0.08               |
| Harvesting                                    | 2                     | -112 (1280)   | -0.3 (1.9)  | -0.7 (2.3)  | 2000 $\pm$ 40                                  | ND <sup>f</sup>                       | ND, ND, ND       | 1.8                |
| Opening of<br>the reactor                     | 3                     | 2278 (3588)   | 146 (1.9)   | 142 (6.5)   | 1100 $\pm$ 40                                  | ND                                    | ND, ND, ND       | 1.0                |
| Cleaning of<br>the reactor <sup>g</sup>       | 4                     | —   | —   | —   | 600 $\pm$ 17                                   | ND                                    | ND, ND, ND       | 2.1                |
| Sieving, mechanical work-up,<br>and packaging | 5                     | 45 (928)  | 21 (2.8)  | 19 (4.9)  | 320 $\pm$ 4.7                                  | <b>11 <math>\pm</math> 1.0</b>        | 41, 18, 41       | 0.04               |
| Lathe machining                               | 6                     | 399 (908)   | 207 (8.2)   | 211 (4.6)   | 770 $\pm$ 13                                   | <b>1.2 <math>\pm</math> 0.50</b>      | 17, 17, 66       | 0.20               |
| Purification part I                           | 7                     | 11 760 (3830)   | -1.9 (8.8)  | -5.2 (12)   | 160 $\pm$ 3.9                                  | ND                                    | ND, ND, ND       | 0.28               |
| Purification part II                          | 8                     | -363 (2948)   | -0.1 (6.2)  | 0.03 (10.1)   | 190 $\pm$ 3.2                                  | <b>0.46 <math>\pm</math> 0.15</b>     | 11, ND, 89       | 0.02               |

Table 3. Continued

| Work Task                    | Location<br>in Fig. 1 | Direct reading instruments   |  |  | SEM analysis                      |                                 |                  |  |
|------------------------------|-----------------------|--|--|--|-----------------------------------|---------------------------------|------------------|--|
|                              |                       | >0.01 µm<br>(CPC) temporal<br>background<br>corrected <sup>a</sup> | >0.5 µm<br>(APS)<br>temporal<br>background<br>corrected <sup>b</sup> | >0.5 µm (APS)<br>spatial<br>background<br>corrected <sup>b</sup> | Total<br>(35 nm–4µm) <sup>c</sup> | All types<br># cm <sup>-3</sup> | Types (1, 2, 3)% | LOD <sup>e</sup><br># cm <sup>-3</sup> |
| Functionalization<br>part I  | 9                     | -325 (3194)  | -2.1 (12.8)  | -0.5 (10.3)  | 290 ± 6.2                         | <b>1.0 ± 0.41</b>               | ND, ND, 100      | 0.1                                    |
| Functionalization<br>part II | 10                    | 1045 (2888)  | -1.2 (8.9)   | -5.8 (16.0)  | 160 ± 4.1                         | ND                              | ND, ND, ND       | 0.11                                   |
| Grinding                     | 11                    | -238 (3152)  | 0.18 (6.7)   | -4.0 (10.9)  | 210 ± 4.1                         | ND                              | ND, ND, ND       | 0.08                                   |

<sup>a</sup>Values in parentheses are the averaged measured backgrounds 3 min before the work task. <sup>b</sup>Values in parentheses are the measured concentrations from the background station instrument. <sup>c</sup>All measured particles, size detection limit: 35 nm (geometric)–4 µm (aerodynamic, 50% cut off, respirable curve). <sup>d</sup>Any particle with visible CNT content. <sup>e</sup>Level of detection (LOD), the upper 95% one sided confidence limits (95% CLs) of the number concentrations of particles in the air were calculated by assuming that the number of particles on the filter could be described using the Poisson distribution. The CL where the observed CNT cluster count was zero is considered to be the LOD. The method for calculating the 95% CL was based on ISO 10312 (1995). <sup>f</sup>Not detected. <sup>g</sup>Due to the short sampling time, the same filter was used for both parts I and II.

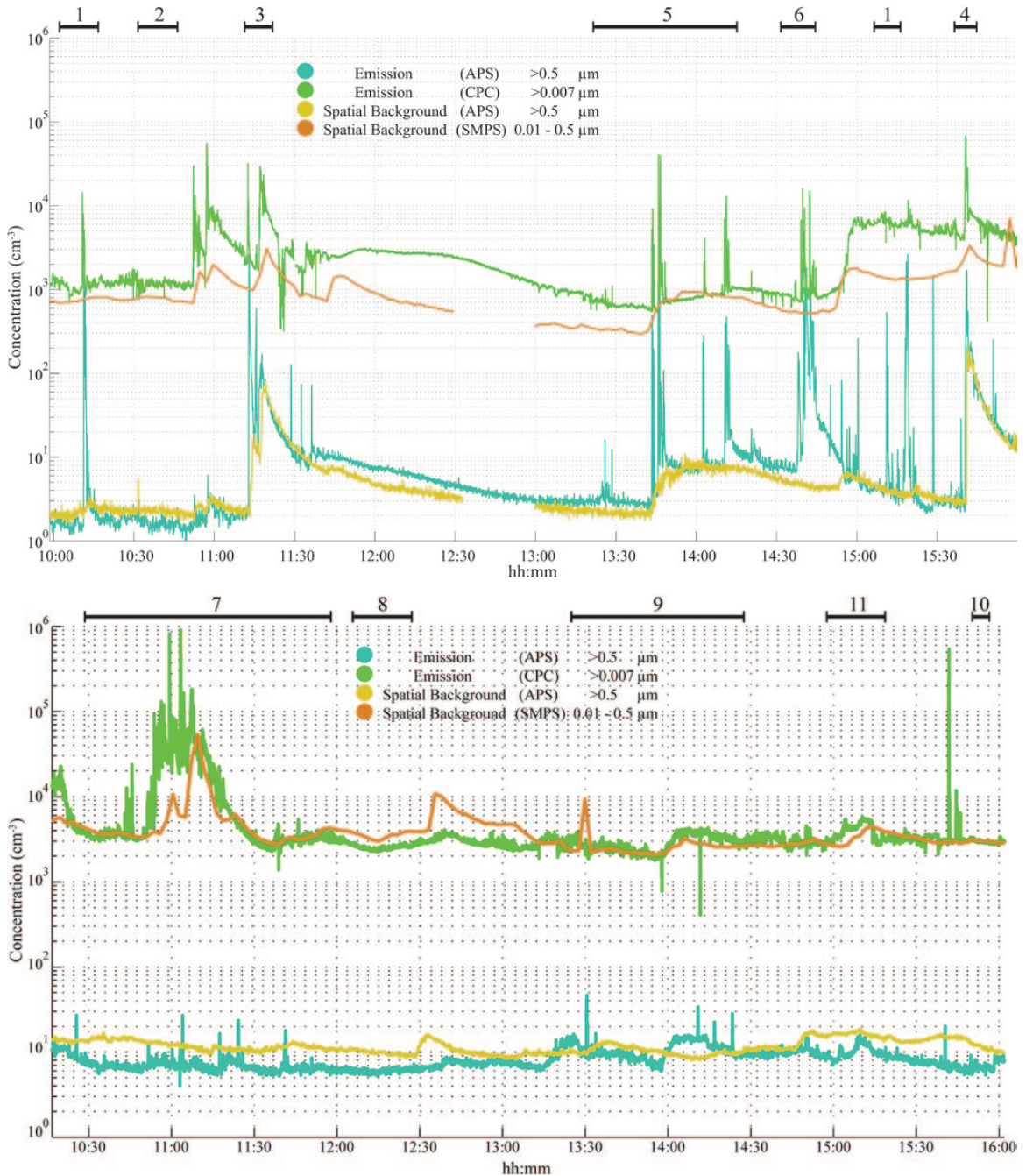


Figure 2 (a) Time series from online instruments measured in the production and sieving laboratories on the first day. Nos. 1–6 refer to Work Tasks: 1. Cleaning of deposits, 2. Harvesting, 3. Opening of the reactor, 4. Cleaning of the reactor, 5. Sieving, 6. Lathe machining. The numbers also refer to the locations in Table 1 and Fig. 1. (b) Time series from online (DRI) instruments measured in the purification laboratory on the second day. Nos. 7–11 refer to Work Tasks: 7. Purification Part I, 8. Purification Part II, 9. Functionalization Part I, 10. Functionalization Part II, 11. Grinding. The numbers also refer to the locations in Fig. 1.

We classified the CNT-containing particles according to three types. To do this, the length and width of the particles were measured. We defined the length as the longest straight path between any two points of a particle, and the width as the longest path between two points perpendicular to the length. Type 1 includes fibre-shaped CNT-containing particles with an aspect ratio  $>3:1$ . Type 2 contains one or more CNT fibres sticking out from a lump of impurities. In order to be classified as a type 2 particle, the CNTs protruding from the lump of impurities must be longer than 50% of the width of the lump. Type 3 particles contain mostly impurities and CNTs are typically only visible when embedded in the surface of the particles or when sticking out from a main body of impurities.

The number concentration of CNT-containing particles (in  $\text{cm}^{-3}$ ) was calculated from the sampled air volume. The analysis of unexposed blank filters as well as of field blanks showed that the polycarbonate filters used did not contribute particles/fibres in the analysis. Calculations of the 95% confidence interval of the detection limits were based on ISO 10312 (1995). The SEM analysis was performed using a Focused Ion Beam—Scanning Electron Microscope (FIB-SEM, model Nova Nanolab 600, FEI, Hillsboro, USA) at Lund Nanolab, Lund University with an acceleration voltage of 5 kV and a probe current of 20  $\mu\text{A}$ . The track-etched polycarbonate filters were prepared for SEM analysis after air sampling by mounting approximately a quarter of the filter on a silicon wafer and coating the filter surface with platinum. This sampling procedure gives a homogenous coverage of the surface. The samples were initially screened for anomalies and areas which were not representative for the filter—those close to the cutting fringes and the edge of the filter—were omitted from further analysis. Images were acquired at a resolution of 35 nm per pixel at a magnification of 2500, generating an imaged area of 9050  $\mu\text{m}^2$  per image. The imaged areas were chosen at random, excluding the previously mentioned, non-representative areas.

The images acquired were analysed in *ImageJ* (Rasband, W.S., ImageJ, National Institute of Health, Bethesda, Maryland, USA, 1997–2008. Available: <http://rsbweb.nih.gov/ij>). Every particle collected in the selected areas was manually measured, regardless of whether it contained CNTs or not. It was noted whether the analyzed particles did or did not contain visible CNTs. The minimum dimension possible to

accurately measure was equivalent to the resolution of the imaged area (i.e. the width of one pixel, which is 35 nm). For particles in the range of a few pixels (35–100 nm), the contrast may in some cases be too low to distinguish the particle from the filter surface, limiting the detectable size range. CNT-containing particles were identified by the distinct contrast between the CNTs and the carbon impurities within the same particle. Particles suspected of containing CNTs were individually screened at a higher resolution to confirm that they actually contained CNTs. A minimum of 5 images, or a total count of 1500 particles were characterized for each filter sample.

## RESULTS

### Time series data from DRI

The time series from the DRIs from both the emission and background zone measurements in the *production* and *sieving laboratories* during day 1 (Work Tasks Nos. 1–6) are shown in Fig. 2a. Peaks from the emission zone DRIs, CPC ( $>0.01 \mu\text{m}$ ) and APS ( $>0.5 \mu\text{m}$ ), coincide with work tasks performed by the worker, indicating that the increase in particle number concentration is related to the work tasks performed. In most cases, the peaks appear as transient episodes (less than a minute) after which the concentration returns to approximately the background value. However, in some cases the elevated concentration remains for a much longer time and clearly induces an increased background concentration, with the potential of exposure for workers in the far-field area as well (*For example opening of the reactor*; Work Task No. 3). In the large particle range a few unexplained short-lived peaks were identified. These are most likely due to resuspension of coarse particles by movements of the workers between work tasks. During the lunch break period no workers were present in the facility, and no emission peaks were found.

In the *purification laboratory* (Work Tasks Nos. 7–11), the most apparent increase in concentration for  $dp > 0.01 \mu\text{m}$  took place when a furnace was opened at 11:12 during Work Task No. 7 (Fig. 2b). The concentration of the larger particles ( $>0.5 \mu\text{m}$ ) assessed with the emission and background APSS, showed only small fluctuations. Peak emission concentrations in the *purification laboratory* ( $>0.5 \mu\text{m}$ ) were about two orders of magnitude lower compared to those in the *production laboratory*.

### Quantification and classification of CNT-containing particles using electron microscopy

Using scanning electron microscopy (SEM), airborne CNT-containing particles were detected in three out of six work tasks in the *production and sieving laboratories*, and two out of five work tasks in the *purification laboratory* (Table 3). In general, CNT-containing particles were a small fraction of the total number of particles detected with SEM (respirable fraction). The highest emissions of CNT-containing particles in the *production laboratory* were found for Work Task No. 5, *Sieving mechanical work-up and packaging* ( $11 \text{ cm}^{-3}$ ) and in the *purification and sieving laboratory* for Work Task No. 9, *Functionalization Part I* ( $1.0 \text{ cm}^{-3}$ ).

Hedmer *et al.* (2014) carried out full-shift PBZ measurements from each laboratory during the same study and found mean values for 2 days of measurements of  $1.3 \text{ cm}^{-3}$  (*production and sieving laboratory*) and  $0.07 \text{ cm}^{-3}$  (*purification laboratory*). By adjusting every work task for its duration, we reconstructed full-shift average concentrations from the task-based emission measurements alone. The reconstructed concentrations of CNT-containing particles were  $1.5$  and  $0.2 \text{ cm}^{-3}$ . The good agreement in the *production and sieving laboratory* suggests that the concentrations in the emission zone were representative for the breathing zone exposure. A three times higher reconstructed concentration from the emission measurements in the *purification laboratory* compared to the PBZ exposure concentration measured is reasonable, as some of the emission sampling was carried out inside hoods and thus may have overestimated the breathing zone exposure. From this analysis, it was also assessed that Work Task No. 5, *Sieving, mechanical work-up, and packaging*,

was responsible for more than 85% of the full-shift PBZ exposure in terms of number of CNT-containing particles in the *production and sieving laboratory*.

From the SEM analysis, it was clear that the CNT-containing particles occurred in a variety of shapes and sizes. The CNT-containing particles ( $N = 338$ , sum for full campaign) counted from the measurements were classified into three types based on the general morphology and size of the particle and the amount of CNTs that it contained (Fig. 3). Type 1 consists of fibre-shaped CNT particles with an aspect length:width ratio  $>3:1$ . Each of these particles typically contained 1–15 individual CNTs stuck parallel to each other. It should be noted that we included all particles fulfilling this criteria, rather than just particles with a length  $>5 \mu\text{m}$ , as in the WHO criteria. The amount of impurities was non-existent or low for this particle type. The average length and width of type 1 particles were  $1.66$  and  $0.26 \mu\text{m}$ , respectively.

Type 2 contains one or more CNT fibres sticking out from a lump of impurities. In order to be classified as a type 2 particle, the CNTs protruding from the lump of impurities should be longer than 50% of the width of the lump. The average length and width of type 2 particles were  $2.05$  and  $1.02 \mu\text{m}$ , respectively. These particles typically contained 5–20 individual CNTs.

Type 3 particles contain mostly impurities and CNTs are only visibly embedded in the surface of the particles or sticking out from a main body of impurities. The average length and width of type 3 particles were  $2.61$  and  $1.69 \mu\text{m}$ , respectively. Type 3 particles contained between 1–30 CNTs.

Based on all the particles counted in the emission samples in the study, the following distribution of particle

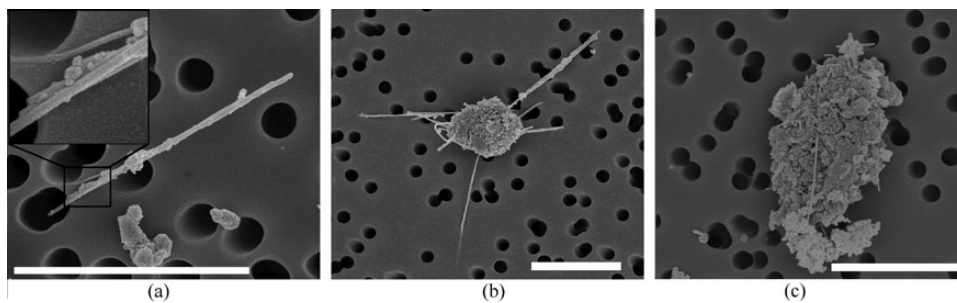


Figure 3 SEM images of different types of airborne CNT-containing particles: (a) type 1 insert shows several strands of CNTs building up the larger structure, (b) type 2, and (c) type 3. The scale bar in each image equals  $3 \mu\text{m}$ . The overall time weighted distribution of the different types was as follows: type 1: 37%; type 2: 22%; type 3: 41%.

types was found: type 1: 37%, type 2: 22%, and type 3: 41%. This was similar to both Task No. 5 *Sieving, mechanical workup, and packaging* (Table 3) and the full-day breathing zone sample from the production lab. (type 1: 35%, type 2: 22%, and type 3: 43%). There was a strong variation in particle type distribution between work tasks.

In Fig. 4, the particle size distributions from SEM analysis for total number of particles counted and CNT-containing particles is given for the full-shift PBZ sample on day 2 in the *production and sieving laboratory*. The length and width distributions of the total number of respirable particles (including CNT-containing particles) counted are relatively narrow, peaking between 100 and 200 nm. In comparison, the length distribution of CNT-containing particles is shifted towards much larger particles, peaking around 1–2  $\mu\text{m}$ . Thus, the size overlap between the total counted particles and the CNT-containing particles is small: 1.6% of the particles counted with SEM contained CNTs.

#### Emissions and size distributions from different work tasks and comparison between SEM and DRIs

Table 3 shows average background adjusted emission concentrations from the DRIs for each work task within the two size ranges. These values can be compared with both the total and the CNT-containing number concentrations derived from the SEM analysis (respirable fraction). No background adjustment

was available for SEM. Since the size ranges in which particles detected are different, the absolute numbers differ. The total concentration detected with SEM ( $>0.03 \mu\text{m}$ ) was typically lower than the total concentration from the CPC ( $>0.01 \mu\text{m}$ ) which is reasonable, as the detection efficiency using SEM starts to drop below 100 nm.

Size distribution of particle emissions from different work tasks were studied using direct reading measurements (APS; time resolved size distributions in Fig. S1) and offline measurements from filter analysis using SEM. A comparison between the two techniques show relatively good agreement both in terms of particle sizes and absolute concentration in the size range  $>0.7 \mu\text{m}$  (Fig. 5a, c, e). A shift towards larger particle sizes indicating high concentrations of mechanically generated particles from the process is found for *Cleaving of deposits* (Work Task No. 2).

#### *Sieving, mechanical work-up, and packaging* (Work Task No. 5)

The DRI data shows that the sieving of CNTs resulted in sharp, short-lived (1–10 s) strong emission peaks that could be related to the process both in the small particle range ( $>0.01 \mu\text{m}$ ) and in the larger particle range ( $>0.5 \mu\text{m}$ ) (Fig. 2a). For the APS ( $>0.5 \mu\text{m}$ ), there was also a clear increase in average emission concentration both for spatial and temporal background

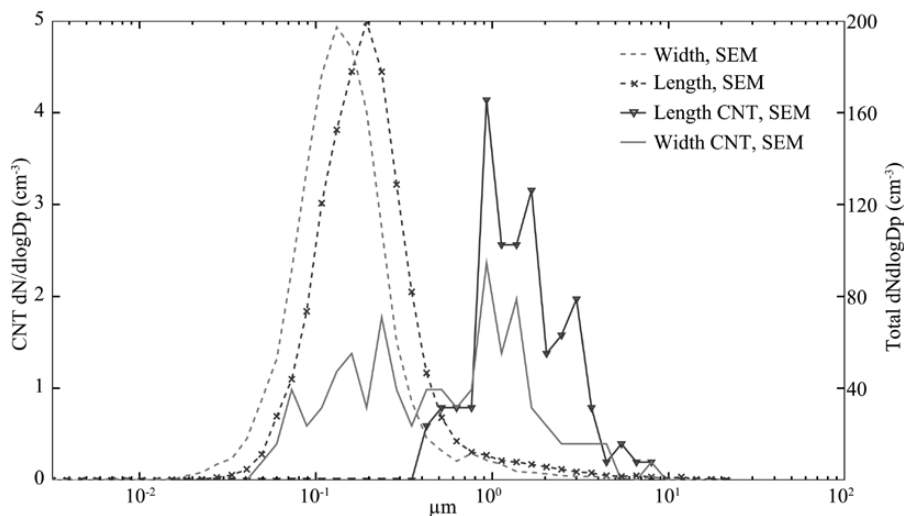


Figure 4 Number size distributions based on particle length and width for SEM total particles and CNT-containing particles (both sampled as respirable fractions). Full-day measurement on day 2 from the worker's breathing zone during work carried out in the production laboratory and sieving laboratories.

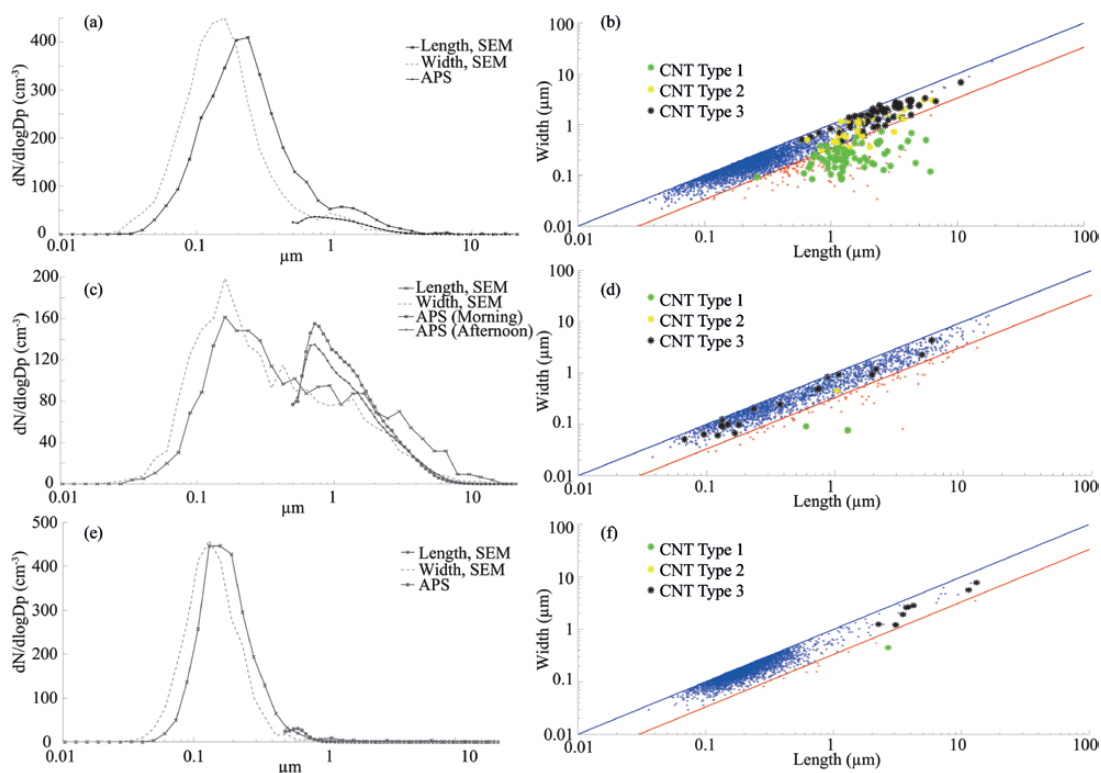


Figure 5 (a, c, and e) Length and width distribution of total particle number concentrations from the SEM analysis and APS aerodynamic particle size distribution. (b, d, and f) Length versus width of measured particles from SEM analysis. Red: non-CNT-containing particles with aspect ratio >3:1; Blue: non-CNT-containing particles with aspect ratio <3:1; Green: CNT-containing particles of type 1; Yellow: CNT-containing particles of type 2; Black: CNT-containing particles of type 3. (a, b) Sieving, mechanical work-up and packaging (Work Task No. 5). (c, d) Cleaving of deposits (Work Task No. 1). (e, f) Purification part II (Work Task No. 8).

adjustment (19 and  $21 \text{ cm}^{-3}$ , respectively Table 3). The concentration of CNT-containing particles was high  $11 \text{ cm}^{-3}$  and Type 1 dominated with 40%. The CNT-containing particles (Fig. 5b) occurred almost exclusively as particles with lengths greater than  $0.5 \mu\text{m}$  (up to  $10 \mu\text{m}$ ), while their width varied between  $0.07$  and  $2 \mu\text{m}$ . In this case, the CNT-containing particles were distinctly different from the majority of the non-CNT-containing particles (lengths typically below  $0.5 \mu\text{m}$ ).

The fraction of the released particles that contain CNTs can be estimated by comparing the number concentrations of the CNT-containing particles from SEM with the background adjusted concentrations from the DRIs. For this work task, SEM provided a concentration of  $11 \text{ cm}^{-3}$ , the APS ( $>0.5 \mu\text{m}$ )  $21 \text{ cm}^{-3}$ , and the CPC ( $>0.01 \mu\text{m}$ )  $45 \text{ cm}^{-3}$ . It is therefore reasonable to assume that a large fraction of the emitted particles from the process contained CNTs.

#### *Cleaving of deposits (Work Task No. 1)*

Cleaving of deposits was carried out twice. It resulted in clear emission peaks in the size range  $>0.5 \mu\text{m}$  (APS). The temporal background adjusted emission concentrations ( $>0.5 \mu\text{m}$ ) were  $53$  and  $93 \text{ cm}^{-3}$  on the two occasions, respectively. Increases in the smaller particle range (as measured by the CPC) were less obvious. The concentration of CNT-containing particles was  $1.6 \text{ cm}^{-3}$ . That is, only a small fraction of the emitted particles from the process contained CNTs. The CNT-containing particles (Fig. 5d) were evenly distributed over a large size range (length =  $0.07$ – $7 \mu\text{m}$ , width =  $0.05$ – $2 \mu\text{m}$ ) and roughly similar to the distribution of the total counted particles. Type 3 particles dominated these emissions (82%).

#### *Lathe machining (Work Task No. 6)*

Lathe machining resulted in the highest emissions of particles  $>0.5 \mu\text{m}$  ( $207 \text{ cm}^{-3}$ ). The concentration

derived from the SEM filter was relatively high ( $770\text{ cm}^{-3}$ ). A moderate concentration of CNT-containing particles ( $1.2\text{ cm}^{-3}$ ) was detected on the SEM samples. Although lathe machining did not involve work with material containing CNTs, it is possible that some CNT-containing particles from the high emissions during sieving 30 min earlier were still airborne. Another possibility is that CNT-containing dust was re-suspended during the operations taking place in connection with lathe machining. The fraction of Type 1 CNT particles was lower for lathe machining compared to sieving (17 versus 41%).

#### *Harvesting (Work Task No. 2)*

Harvesting did not result in any clear emission peaks in either size range with the DRIs. However, the SEM analysis showed a very high concentration,  $2000\text{ cm}^{-3}$ . This exceeds the total CPC concentration  $>0.01\text{ }\mu\text{m}$  and is difficult to explain. No CNT-containing particles were detected at this work task.

*Opening and cleaning of the reactor (Work Tasks Nos. 3, 4)*  
When opening the reactor, high number concentrations of particles in both size ranges were emitted ( $2278\text{ cm}^{-3}$  for  $>0.01\text{ }\mu\text{m}$ ,  $146\text{ cm}^{-3}$  for  $>0.5\text{ }\mu\text{m}$ ). As pointed out previously, these emissions affected the background concentration leading to potential far-field exposures for a long period (Fig. 2a). SEM analysis also showed high concentrations ( $1100\text{ cm}^{-3}$ ). Cleaning of the reactor was carried out on day 2 when the DRIs were not available in the production lab, but the SEM analysis showed a high concentration of particles ( $600\text{ cm}^{-3}$ ). Even though these two processes resulted in very high emissions, no CNT-containing particles were detected. The filter samples from these work tasks contained almost exclusively porous soot agglomerates with (geometric) sizes ranging from submicrometer to well above  $30\text{ }\mu\text{m}$ .

#### *Purification laboratory (Work Tasks Nos. 7–11)*

All the work tasks in the *purification laboratory* generated similar size distributions (peaks at around  $200\text{ nm}$ , example in Fig. 5e) and similar concentrations in the SEM analysis ( $150\text{--}300\text{ cm}^{-3}$ ). The background adjusted CPC emission concentrations ( $>0.01\text{ }\mu\text{m}$ ) were negligible for *Functionalization Parts I and II* and *Purification Part II*. It is expected that background

particles, possibly infiltrated from ambient air, were the main source of the particles detected with SEM.

For *Purification Part I* (Work Task No. 7), relatively high emissions were recorded in the  $>0.01\text{ }\mu\text{m}$  range in connection with turning on a high temperature furnace. Since these particles did not affect either the SEM or the APS concentrations, they can be expected to be mainly  $<50\text{ nm}$ . For the APS ( $>0.5\text{ }\mu\text{m}$ ), none of the five work tasks showed average concentrations higher than 10% above the background, although very short-lived relatively small peaks above the background concentrations were identified in the emission zone for *Purification Part I* (Work Task No. 7) and *Functionalization Part I* (Work Task No. 9).

CNT-containing particles were only detected from *Functionalization Part I* (Work Task No. 9;  $1.0\text{ cm}^{-3}$ ) and *Purification Part II* (Work Task No. 8;  $0.46\text{ cm}^{-3}$ ). In both these cases, the CNT-containing particles had lengths longer than  $1\text{ }\mu\text{m}$ ; in that size range they constituted a significant fraction of the detected particles with SEM (Fig. 5f). The most abundant CNT particle type was type 3, constituting 69% of the total amount of CNT particles. Since the emission concentrations from the DRIs were very low for these two work tasks, it is likely that a large fraction of the emitted particles contained CNTs.

## DISCUSSION

### Emissions of CNT-containing particles from different work tasks

In this study, we carried out detailed investigations of particle emissions from a total of 11 work tasks during arc discharge production of MWCNTs. There were strong variations in the total emitted particle concentrations measured in the two size ranges with the DRIs as well as in the total number of particles and CNT-containing particles collected on filters and analysed offline. Emissions of CNT-containing particles were identified with EM for 5 out of the 11 work tasks investigated. CNT-containing particles were also identified on all PBZ filters. The highest CNT-containing emissions were found during open and manual handling of CNT-containing material (*Sieving, mechanical work-up, and packaging*, Work Task No. 5). This was the work task with the longest duration and the distributions of particle types were similar to the full-day personal exposure sample, clearly indicating that

the majority of the personal exposure came from this source.

We also found respirable emissions of CNT-containing material from two other sources in the *production laboratory* (*Cleaving of deposits* and *Lathe machining*, Work Tasks Nos. 1 and 6) and from two work tasks in the *purification laboratory* (*Functionalization Part I* and *Purification Part II*, Work Tasks Nos. 9 and 8). Our emission data of MWCNTs ranged between  $<0.20$  and  $11 \text{ cm}^{-3}$ . When compared with the highest emission level reported by others during manufacturing of MWCNTs, our emission data is higher than what Ogura *et al.* (2011) and Dahm *et al.* (2013) found, but lower than the levels reported by Han *et al.* (2008).

#### Particle types and release mechanisms

Both emission concentrations of CNT-containing particles, and the properties (length, width, degree of purity, etc.) varied strongly between the work tasks. For example, emissions from *Sieving, mechanical work-up, and packaging* had a very high fraction of 'free fibres' (type 1) CNT-containing particles (41%). This is much higher than in several previous studies on CNT emissions from other types of production processes. For example, Tsai *et al.* (2009) reported the release of predominantly clusters of spherical shape with some individual nanoparticles as well as MWCNTs for CVD production of CNTs with a low injector temperature.

On the other hand, *Cleaving of deposits* and *Purification Part II* (Work Tasks Nos. 1 and 8) were dominated by type 2 and type 3 particles, with very few 'free' fibres. However, between these two cases there were also differences. *Cleaving of deposits* included CNT-containing particles distributed over a large size range with lengths and widths similar to the total particles detected with SEM. For *Purification Part II*, though, the emitted CNT-containing particles were much larger in both length and width than the majority of collected particles. Thus, it is hard to draw generalized conclusions regarding the characteristics of the CNT exposures from arc discharge production compared to other manufacturing methods.

It is likely that the material properties and the type of handling affect the amounts of released CNTs as well as the types of particles released. For example, the cleaving of deposits involves high temperatures and

large amounts of energy added to the material, while sieving involves open handling of CNT-containing raw material, with much lower energy input.

Emissions of CNT-containing particles were unexpectedly found during the lathe machining of unreacted graphite (i.e. material that did not contain CNTs). This suggests that the re-suspension of deposited CNT-containing dust may occur. An analysis of surface contamination at this workplace is reported by Hedmer *et al.* (2015).

#### Knowledge gained by combining DRIs and offline EM-based techniques, influence of background concentration

The EM techniques have higher specificity for exposures containing CNTs compared to the DRIs as also shown by Dahm *et al.* (2013). A similar conclusion was obtained by Hedmer *et al.* (2014) when comparing the SEM technique to EC and total dust as exposure metrics. On the other hand, from the time-integrated filter-based SEM technique, only limited understanding can be gained of what specific actions lead to CNT release during a given work task.

This study gives several examples of added value by using the combination of the SEM and DRI techniques. One benefit of highly time-resolved analysis is the identification of emission peaks. This includes the peak concentration relative to the background and the length of the emission peak. Additionally, we could differentiate between short-lived emission events that did not affect the background, and emission events that affected the background for prolonged time leading to potential far-field exposure risks for workers other than the operator of the work task in question.

It is essential to correct for, and understand, the impact of the background concentration at the workplace. Background particles can infiltrate from outdoors (ambient particles) or be generated by indoor activities not related to the current work task. The background particle concentrations and size distributions are determined by a number of factors such as ventilation rates, infiltration from neighboring laboratories, and ambient air and emissions from multiple sources at the actual workplace. The background number concentration  $>0.01 \mu\text{m}$  in the workshop during periods with no activity was  $1000\text{--}2000 \text{ cm}^{-3}$  with no obvious indoor sources. These are likely ambient particles that have penetrated from outdoors.

Temporal and spatial background adjustment was compared for particles larger than 0.5  $\mu\text{m}$ . For strong sources these two approaches showed very good agreement, while for cases where the emission concentration was small compared to the background, they differed more. Emissions more than 20% above background were found for four sources in the size range  $>0.01 \mu\text{m}$ ; two of these also released CNT-containing particles. Five sources showed emissions clearly above the background in the size range  $>0.5 \mu\text{m}$ ; four of these led to emissions of CNT-containing particles detected with SEM, suggesting a stronger connection between emissions of particles  $>0.5 \mu\text{m}$  and CNT-containing particles compared to emissions in the size range  $>0.01 \mu\text{m}$ .

The combined DRI and SEM techniques also provided evidence for particle emissions that did not contain CNTs but were released during the work tasks studied. By comparing the number concentration of CNT-containing particles with the total concentration of emitted particles from each source in the two size ranges from the DRIs (Table 3), we could roughly estimate the fraction of the emitted particles that contained CNTs. For the *Sieving work task* and *Functionalization Part I* and *Purification Part II* (Work Tasks Nos. 5, 8, and 9), CNT-containing particles may have contributed to a substantial fraction of the emitted particles, possibly as much as ~50%. The uncertainty in this number is quite high due to a high background concentration, particularly for the size range  $>0.01 \mu\text{m}$ . For the case of *Cleaving of deposits* (Work Task No. 1), the fraction of CNT-containing particles was  $<10\%$ . During this task, the majority of released particles may have been generated when cutting through the non-CNT-containing 'shell' of the deposits, or emitted from the saw blade. For *Lathe machining* (Work Task No. 6), the CNT-containing particles were an even smaller fraction, as expected since no CNT-containing material was handled.

Even though *Opening of the reactor* and *Purification Part I* (Work Tasks Nos. 3 and 7) had the highest emissions of  $>0.01 \mu\text{m}$  particles, no CNT-containing particles could be detected. In the case of opening the reactor, the emitted particles were soot/graphite particles. In *Purification Part I*, high concentrations of particles were released ( $<0.01 \mu\text{m}$ ), but the emitted particles could not be detected with SEM due to their small size. Most likely these ultrafine particles were

generated by thermal processes in the case of heating up and opening the oven in the *purification laboratory*.

For very small particles below about 40 nm (geometric diameter), it is only the SMPS and CPC that can detect the particles. The CPC detects the entire particle size range of interest ( $>0.01 \mu\text{m}$ ), but because of the usually high background in this size range, CNT-containing particles may be hidden in the noise. With the APS in the large particle range ( $>0.5 \mu\text{m}$ ), emissions are often more clear. It seems that the APS in most of the cases measures particle size distributions and number concentrations above 0.7  $\mu\text{m}$  that are similar to the SEM distributions. The underestimation of particles smaller than about 0.7  $\mu\text{m}$  depends on the decreasing counting efficiency of the APS in this range.

#### SEM method: implications for legislative limits and exposure metrics

The number concentration of fibre-containing particles is likely the most important exposure metric for fibre-shaped nanoparticles with high aspect ratios. Today there is no consensus on how CNTs collected with a filter-based sampling methodology should be counted in EM analysis. According to the WHO's standard fibre counting criteria that are used, for example, in asbestos counting (1986, 1997), a particle is defined as a fibre if it has a length  $>5 \mu\text{m}$ , a width  $<3 \mu\text{m}$ , and an aspect ratio  $>3:1$ . In addition, fibres are counted separately as if the carrier particles did not exist.

Typically all three particle classes found in this study contained a relatively high number of individual CNTs (1–30) with length  $<5 \mu\text{m}$  and we assessed that it was not possible to practically count every single CNT. Thus, we decided not to follow the standard fibre counting criteria. If the length criteria were followed, less than 1% of our total counted CNT-containing particles would have been defined as fibres.

Several previous studies that followed the WHO counting rules quantified no or few CNTs (Bello *et al.*, 2009; Lee *et al.*, 2010) and may therefore have underestimated the presence of CNTs in workplace air. Moreover, shorter MWCNTs (length  $<5 \mu\text{m}$ ) have been shown to penetrate the visceral pleura in rats (Mercer *et al.*, 2010), to cause pulmonary inflammatory effects and fibrosis (Mercer *et al.*, 2011; Porter *et al.*, 2013) and bronchoalveolar inflammation and

thickening of the alveolus septum in rats, indicative of interstitial fibrosis (Pauluhn, 2010b). These adverse health effects may be caused by other CNT characteristics than fibre lengths, and demonstrate that the standard fibre counting criteria is not applicable for all CNTs. It is not known what happens to the CNT agglomerates deposited in the lungs (e.g. deagglomeration may occur with the subsequent release of single CNTs). More research on lung deposition and particularly the fate of agglomerated CNTs in lung fluid is needed.

Recently it was proposed that EC may be a usable metric for CNT exposure (Dahm *et al.*, 2012; NIOSH, 2013). Our recent publication reported that the EC exposure metric is both too insensitive and unspecific to be used as a generic exposure metric for CNT exposures during arc discharge production (Hedmer *et al.*, 2014). For example in *Cleaning of the reactor* (Work Task No. 4), no CNTs were detected while the EC concentration was very high ( $550 \mu\text{g}/\text{m}^3$ ). SEM analysis is time consuming, expensive, and not at all as commercially available as EC analysis, but it is very important that the analytical method used to quantify exposures to CNTs has high selectivity and sensitivity to CNTs.

A further development of the SEM method is needed to decrease the analysis time and thereby the costs of the analysis. Computer software is available for image analysis with automatic counting of objects in SEM on substrates without pores. There is also ongoing research to develop computer software that automatically can perform the image analysis of fibre-shaped objects on filter samples. Thus, in the near future it will be possible to automatically, quickly, more easily, and inexpensively count CNTs in EM, which will ease the establishment of a standardized protocol for counting criteria of CNTs. The SEM method we developed can be applied for analysis of all fibre-shaped nano-objects, and their aggregates and agglomerates (NOAAs)  $>100 \text{ nm}$  with high aspect ratios that have structural similarities with asbestos (e.g. metal and semiconductor nanowires).

Online techniques for the selective detection of particles from different processes are deeply needed. An example is the application of time-resolved aerosol mass spectrometry for the selective detection of metals and different types of carbonaceous particles (Onasch *et al.*, 2012; Nilsson *et al.*, 2013).

### Recommendations to the company

For CNT exposures, the precautionary principle must be applied until the toxicological effects of CNT exposure have been evaluated. In practice, this means enclosed handling in combination with a high level of control measures and a high degree of use of personal protection equipment (PPE). Thus, the workers in the facility were assessed to have higher exposure than necessary due to lack of PPE as well as in engineering controls. Dry CNT powder should not be openly handled in the facility without any engineering controls, such as ventilated enclosures (Schulte *et al.*, 2012). During all open handling of CNTs in the facility, respiratory protection must be used. To protect the workers more efficiently, PPEs such as coveralls, hoods, and shoe protection are needed especially in the *production laboratory* to prevent dermal exposure and to inhibit the CNT dust spreading in the workplace. The engineering controls used were assessed and found not to be sufficient for reducing the CNT exposure. For example, the *production laboratory* was not located in a closed area since it was part of a larger room that was used for other purposes such as storing. The *production laboratory* was connected via stairs to other rooms in the building without any airtight sluice. This means that airborne CNT-containing particles could be present in other rooms in the building and thereby cause exposure to unprotected workers. Moreover, the office used by the production workers was located next to the *sieving laboratory*, and since the same shoes were worn in both the *production laboratory* and *sieving laboratory* as in the office, there could be a high risk that the floor in the office was contaminated with CNT dust.

### Limitations

It should be pointed out that the data obtained may not be directly generalizable to other CNT manufacturing methods (such as the more commonly used CVD method) and to workplaces with stricter engineering control systems. Due to the use of respirable particle size selection, this study does not give a full image of the particle emissions that occur during the different work tasks since particles with aerodynamic diameters larger than the respirable size limit are expected to be released into the air as well. This study focuses on the particles with the highest probability to reach the pulmonary region and thus does not consider particles

that most likely are deposited above the pulmonary region, such as large ( $d_{ae} > 4\mu\text{m}$ ) agglomerated particles. Hedmer *et al.* (2015) present microscopy data from cascade impactor sampling without preselection from the same campaign.

### CONCLUSIONS

The emissions of CNTs during specific work tasks performed in arc discharge production and purification in a small-scale factory were characterized. In addition, a method for SEM analysis of CNT-containing particles on filter samples was developed that makes it possible to classify CNT-containing particles into different types based on their morphology. Particles containing CNTs were found on emission filter samples from five out of the eleven work tasks investigated. Full-shift PBZ exposures exceeded the proposed OELs. By far, the highest contribution (>85%) was from manual handling of CNTs in powder form during *Sieving, mechanical work-up, and packaging*. The morphology of the CNT-containing particles was diverse; free CNT fibres constituted 37% of the total CNT-containing particles. However, the type distribution and characteristics of the CNT-containing particles varied strongly between work tasks.

Data from DRIs provided complementary information on: (i) the background adjusted emission concentration of total particles from each work task in different particle size ranges, (ii) the identification of the key procedures in each work task that lead to emission peaks, (iii) the identification of emission events that affect the background, thereby leading to potential far-field exposures for workers other than the operator of the work task, and (iv) when combined with SEM analysis, the fraction of particles emitted from each source that contains CNTs could be estimated. Thus, this study confirms that a combination of online time-resolved instrumentation and time-integrated filter sampling methods is needed in order to achieve a full evaluation of particle emissions that occur during the production and purification of CNTs. A standardized/harmonized method for the EM analysis of airborne CNTs is urgently needed since only filter-based sampling methods in combination with EM analysis are currently selective and sensitive enough for measuring CNTs. The SEM method presented in this study could form the basis for such a harmonized protocol for the counting of CNTs.

### SUPPLEMENTARY DATA

Supplementary data can be found at <http://annhyg.oxfordjournals.org/>.

### FUNDING

The project was funded by the Swedish Council for Working Life and Social Research (FORTE Grant Nbr. 2009-1291), AFA Insurance, Grant Nbr. 130122, and The European Commission 7th Framework Programme (NANoREG), Grant Agreement Number 310584.

### ACKNOWLEDGEMENTS AND DISCLAIMER

The study was carried out at the METALUND and NanoLund Competence Centres at Lund University, Sweden. The company at which the measurements were conducted approved of the manuscript before submission and no relations that could appear to influence the paper could be identified.

### REFERENCES

- Bello D, Hart AJ, Ahn K *et al.* (2008) Particle exposure levels during CVD growth and subsequent handling of vertically-aligned carbon nanotube films. *Carbon*; 46: 974–7.
- Bello D, Wardle BL, Yamamoto N *et al.* (2009) Exposure to nanoscale particles and fibers during machining of hybrid advanced composites containing carbon nanotubes. *J Nanoparticle Res*; 11: 231–49.
- BSI. (2007) *Nanotechnologies – part 2: guide to safe handling and disposal of manufactured nanomaterials*. London, UK: British Standards Institute.
- Dahm MM, Evans DE, Schubauer-Berigan MK *et al.* (2012) Occupational exposure assessment in carbon nanotube and nanofiber primary and secondary manufacturers. *Ann Occup Hyg*; 56: 542–56.
- Dahm MM, Evans DE, Schubauer-Berigan MK *et al.* (2013) Occupational exposure assessment in carbon nanotube and nanofiber primary and secondary manufacturers: mobile direct-reading sampling. *Ann Occup Hyg*; 57: 328–44.
- Gamaly EG, Ebbesen TW. (1995) Mechanism of Carbon Nanotube Formation in the Arc-Discharge. *Phys Rev B*. 52: 2083–9.
- Gustavsson P, Hedmer M, Rissler J. (2011) Carbon nanotubes – Exposure, toxicology and protective measures in the work environment. *Swedish Work Environment Authority Report* 2011.
- Han JH, Lee EJ, Lee JH *et al.* (2008) Monitoring multiwalled carbon nanotube exposure in carbon nanotube research facility. *Inhal Toxicol*; 20: 741–9.

- Hedmer M, Kåredal M, Gustavsson P *et al.* (2013) The Nordic Expert Group for criteria documentation of health risks from chemicals. 148. Carbon nanotubes. *Arbete och Hälsa*; 47: 1–238.
- Hedmer M, Isaxon C, Nilsson PT *et al.* (2014) Exposure and emission measurements during production, purification, and functionalization of arc-discharge-produced multi-walled carbon nanotubes. *Ann. Occup Hyg*; 58: 355.
- Hedmer M, Ludvigsson L, Isaxon C *et al.* (2015) Detection of carbon nanotubes and carbon nanodiscs on workplace surfaces in a small-scale producer. *Ann Occup Hyg*; 53: 836.
- IFA. (2014). Criteria for assessment of the effectiveness of protective measures. Available at <http://www.dguv.de/ifa/Fachinfos/Nanopartikel-am-Arbeitsplatz/Beurteilung-von-Schutzmaßnahmen/index-2.jsp>. Accessed 5 October 2015.
- Iijima S. (1991) Helical microtubules of graphitic carbon. *Nature*; 354: 56–8.
- ISO 10312. (1995) *Ambient air—determination of asbestos fibres—direct transfer transmission electron microscopy method*. Technical Committee ISO/TC 146, Air quality, Subcommittee SC 3, Ambient atmospheres.
- Jones AD. (2005) Thoracic size-selective sampling of fibres: performance of four types of thoracic sampler in laboratory tests. *Ann Occup Hyg*; 49: 481–92.
- Kumar M, Ando Y. (2010) Chemical vapor deposition of carbon nanotubes: a review on growth mechanism and mass production. *J Nanosci Nanotechnol*; 10: 3739–58.
- Köhler A, Som C, Helland A *et al.* (2008) Studying the potential release of carbon nanotubes throughout the application life cycle. *J Clean Prod*; 16: 927–37.
- Lee J, Mahendra S, Alvarez PJ. (2010) Nanomaterials in the construction industry: a review of their applications and environmental health and safety considerations. *ACS Nano*; 4: 3580–90.
- Liu Y, Kumar S. (2014) Polymer/carbon nanotube nano composite fibers—a review. *ACS Appl Mater Interfaces*; 6: 6069–87.
- Ma-Hock L, Strauss V, Treumann S *et al.* (2013) Comparative inhalation toxicity of multi-wall carbon nanotubes, graphene, graphite nanoplatelets and low surface carbon black. *Particle Fibre Toxicol*; 10: 23.
- Ma-Hock L, Treumann S, Strauss V *et al.* (2009) Inhalation toxicity of multiwall carbon nanotubes in rats exposed for 3 months. *Toxicol Sci*; 112: 468–81.
- Maynard AD, Baron PA, Foley M *et al.* (2004) Exposure to carbon nanotube material: aerosol release during the handling of unrefined single-walled carbon nanotube material. *J Toxicol Environ Health Part A*; 67: 87–107.
- Mercer RR, Hubbs AF, Scabilloni JF *et al.* (2011) Pulmonary fibrotic response to aspiration of multi-walled carbon nanotubes. *Particle Fibre Toxicol*; 8: 21.
- Mercer RR, Hubbs AF, Scabilloni JF *et al.* (2010) Distribution and persistence of pleural penetrations by multi-walled carbon nanotubes. *Particle Fibre Toxicol*; 7: 28.
- Methner M, Hodson L, Geraci C. (2010) Nanoparticle emission assessment technique (NEAT) for the identification and measurement of potential inhalation exposure to engineered nanomaterials—part A. *J Occup Environ Hyg*; 7: 127–32.
- Muller J, Huaux F, Moreau N *et al.* (2005) Respiratory toxicity of multi-wall carbon nanotubes. *Toxicol Appl Pharm*; 207: 221–31.
- Murphy FA, Poland CA, Duffin R *et al.* (2011) Length-dependent retention of carbon nanotubes in the pleural space of mice initiates sustained inflammation and progressive fibrosis on the parietal pleura. *Am J Pathol*; 178: 2587–600.
- Nilsson PT, Isaxon C, Eriksson AC *et al.* (2013). Nano-objects emitted during maintenance of common particle generators: direct chemical characterization with aerosol mass spectrometry and implications for risk assessments. *J Nanoparticle Res*; 15: 2052.
- NIOSH. (2013) Current Intelligence Bulletin 65: occupational exposure to carbon nanotubes and nanofibers. Available at <http://www.cdc.gov/niosh/docs/2013-145/>. Accessed 2 December 2015.
- NIOSH. (2013) Occupational exposure to carbon nanotubes and nanofibres. Available at <http://www.cdc.gov/niosh/docs/2013-145/pdfs/2013-145.pdf>. Accessed 24 May 2013.
- Ogura I, Sakurai H, Mizuno K *et al.* (2011) Release potential of single-wall carbon nanotubes produced by super-growth method during manufacturing and handling. *J Nanoparticle Res*; 13: 1265–80.
- OH Learning. (2010) W504-fibre counting. Available at [http://www.ohlearning.com/Files/Extracted\\_Files/38/W504coursematerial/JD33%20v1-0%2010Apr10%20W504%20Fibre%20counting.ppt#385,1,W504-fibre-counting](http://www.ohlearning.com/Files/Extracted_Files/38/W504coursematerial/JD33%20v1-0%2010Apr10%20W504%20Fibre%20counting.ppt#385,1,W504-fibre-counting). Accessed 16 September 2014.
- Onasch TB, Trimborn A, Fortner EC *et al.* (2012). Soot particle aerosol mass spectrometer: development, validation, and initial application. *Aerosol Sci Technol*; 46: 804–17.
- Pauluhn J. (2010a) Multi-walled carbon nanotubes (Baytubes): approach for derivation of occupational exposure limit. *Regulatory Toxicol Pharmacol*; 57: 78–89.
- Pauluhn J. (2010b) Subchronic 13-week inhalation exposure of rats to multiwalled carbon nanotubes: toxic effects are determined by density of agglomerate structures, not fibrillar structures. *Toxicol Sci*; 113: 226–42.
- Porter DW, Hubbs AF, Chen BT *et al.* (2013) Acute pulmonary dose-responses to inhaled multi-walled carbon nanotubes. *Nanotoxicology*; 7: 1179–94.
- Sanchez VC, Pietruska JR, Miselis NR *et al.* (2010) Biopersistence and potential adverse health impacts of fibrous nanomaterials: what have we learned from asbestos? *Wiley Interdisciplinary Rev Nanomed Nanobiotechnol*; 1: 511–29.
- Sargent LM, Porter DW, Staska LM *et al.* (2014) Promotion of lung adenocarcinoma following inhalation exposure to multi-walled carbon nanotubes. *Particle Fibre Toxicol*; 11: 3.

- Schulte PA, Kuempel ED, Zumwalde RD *et al.* (2012) Focused actions to protect carbon nanotube workers. *Am J Ind Med*; 55: 395–411.
- Takaya M, Ono-Ogasawara M, Shinohara Y *et al.* (2012) Evaluation of exposure risk in the weaving process of MWCNT-coated yarn with real-time particle concentration measurements and characterization of dust particles. *Ind Health*; 50: 147–55.
- Tsai SJ, Hofmann M, Hallock M *et al.* (2009) Characterization and evaluation of nanoparticle release during the synthesis of single-walled and multiwalled carbon nanotubes by chemical vapor deposition. *Environ Sci Technol*; 43: 6017–23.
- WHO. (1986) *Asbestos and other natural mineral fibres. Environmental health criteria, no. 53.* Geneva: World Health Organization.
- WHO. (1997) *Determination of airborne fibre number concentrations: a recommended method, by phasecontrast optical microscopy (membrane filter method).* Geneva: World Health Organization.
- Wohlleben W, Brill S, Meier MW *et al.* (2011) On the lifecycle of nanocomposites: comparing released fragments and their in-vivo hazards from three release mechanisms and four nanocomposites. *Small*; 7: 2384–95.